Organocatalyzed Atom Transfer Radical Polymerization Catalyzed by Core Modified *N*–Aryl Phenoxazines Performed under Air

Blaine McCarthy, **Garret M. Miyake**[*]

Department of Chemistry, Colorado State University, Fort Collins, Colorado 80523-1872, United States of America

Abstract

Organocatalyzed atom transfer radical polymerization (O-ATRP) was performed under air using core modified *N*-aryl phenoxazines as photoredox catalysts (PCs) to synthesize poly(methyl methacrylate) in a controlled fashion with initiator efficiency ($I^* = M_{\mathrm{n,theo}}/M_\mathrm{n} \times 100$) ranging from 84 to 99% and dispersity being ~1.2–1.3. Reduction of the reaction vial headspace was key for enabling the polymerization to proceed in a controlled fashion, as has been observed in Cu catalyzed controlled radical polymerizations. The ability to synthesize block copolymers and turn the polymerization on and off via manipulation of the light source was demonstrated. Six core modified *N*-aryl phenoxazines were able to catalyze O-ATRP under air, albeit with most PCs achieving I^*s ~ 5% lower under air compared to when the reaction was performed under nitrogen.

Grapgical Absrtact

Controlled radical polymerization (CRP) methods mediated by photoredox catalysis have enabled the synthesis of polymeric materials with complex functionality and architecture under mild conditions that can be controlled through the manipulation of a light source.[1,2] The ability to control the polymerization spatially and temporally using a light source

---

enables the application of these methods for photolithography and 3D-printing.[3,4] One barrier hindering the potential of photoredox catalyzed CRPs is the inability to perform these reactions under air. This challenge arises because oxygen (~20% of air) can quench propagating radical species[5] and is a triplet in the ground state which can engage in triplet–triplet annihilation with other triplet species, in particular photoredox catalysts (PCs) that operate from a triplet excited state.[6]

Significant advances have been made in the development of oxygen tolerant photoredox catalyzed CRPs, but the majority of this work has focused on derivatives of reversible addition– fragmentation chain transfer polymerization.[7] Less attention has been paid to photoredox catalyzed variants of atom transfer radical polymerization (ATRP). Our interest in photoredox catalyzed variants of ATRP originated from our work on the development of organocatalyzed atom transfer radical polymerization (O-ATRP). Our group has investigated visible-light driven O-ATRP systems using organic dyes including perylene,[8] N,N-diaryl dihydrophenazines,[9–12] and N-aryl phenoxazines[13–15] as PCs. Despite the progress of our group and others[16–24] developing O-ATRP systems,[25,26] little progress has been made developing oxygen tolerant variants.

In copper catalyzed ATRP, oxygen tolerance has been achieved through a variety of methods which often involve regeneration of the activating Cu(I)/Cu(0) catalyst after it has been oxidized to form Cu(II)/Cu(I) by oxygen.[7] More recently, it has been suggested that the initiator also plays a role in oxygen consumption.[27] In addition to regenerating the catalyst through addition of exogenous reagents or the use of external stimuli, the volume of air available to the reaction mixture has also been identified as a key parameter. For example, increasing the volume of headspace of air in the reaction vessel for Cu-catalyzed ATRP slowed the polymerization such that performing the reaction in a flask open to air inhibited the reaction.[28] Similarly, in Cu-catalyzed reversible deactivation radical polymerizations performed under air, decreasing the reaction vessel headspace increased the rate of polymerization while retaining controlled characteristics such that elimination of vial headspace led to the most rapid controlled polymerization.[27] The decrease in polymerization kinetics with increasing headspace volume was attributed to the increased amount of oxygen available to oxidize the activating species.

In our previous work we observed that the O-ATRP of methyl methacrylate (MMA) catalyzed by perylene, *N,N*-diaryldihydrophenazines, *N*-aryl phenoxazines, or core modified *N*-aryl phenoxazines (such as PC 1, Table 1) performed under air resulted in an uncontrolled polymerization or no polymerization.[8,9,13] However, these reactions were performed in 20 mL scintillation vials with ~18 mL of headspace of air. Inspired by previous ATRP reports demonstrating the beneficial effects of reducing the volume of reaction vial headspace for polymerizations performed under air,[27,28] we sought to determine if this would have a similar effect on O-ATRP systems. To study the effect of air on O-ATRP, the O-ATRP of MMA catalyzed by 1 was chosen as a model system since PC 1 was previously shown to catalyze O-ATRP under a variety of conditions[13,29,30] for the synthesis of polymers with complex composition[31] and architecture.[32] Minimal reagent purification was performed to enable saturation of air in the reaction mixtures (see Supporting Information for more details).

Performing the O-ATRP of MMA under air in a 20 mL scintillation vial (18.2 mL of headspace) led to only 36% monomer conversion after 24 h (Table 1, run 1). In accordance with our previous results,[13] the poly(methyl methacrylate) (PMMA) synthesized exhibited high dispersity, , (= 1.90) a number-average molecular weight (M_n) which deviated appreciably from the theoretical value as indicated by a low initiator efficiency, I^*, ($I^* = M_{n,theo}/M_n \times 100$) of 50%, and a broad and asymmetric gel-permeation chromatography (GPC) trace (Figure S11), demonstrating that the polymerization was uncontrolled. Reducing the volume of air in the reaction vial had a drastic effect on the polymerization (Table 1, runs 1 and 2). The O-ATRP performed with reduced vial headspace (5.55 mL instead of 18.2 mL) proceeded more rapidly, reaching 69% conversion in 24 h (run 2) rather than 36% conversion (run 1), and exhibited characteristics of a controlled polymerization, producing PMMA with = 1.25 and $I^* = 75\%$. Further reduction of the reaction vial headspace continued to increase the rate of polymerization and the O-ATRP performed in a vial with no headspace reached 68% conversion in 8 h (run 5). All polymerizations performed exposed to 5.55 mL of headspace or less (runs 2–5) led to the synthesis of PMMA with moderate (~ 1.2) and I^* ranging from 75–87%, with the reaction performed in a vial with no headspace (run 5) exhibiting the best overall combination of low (= 1.22) and high I^* ($I^* = 87\%$). Moreover, by performing the polymerization in a vial with no headspace for 26 h high monomer conversion was achieved (95%) while exhibiting controlled characteristics (PMMA = 1.18 and $I^* = 87\%$). Omission of PC (run 7), light (run 8), or initiator (run 9) led to no polymerization or an uncontrolled polymerization.

To further explore the effect of air on the O-ATRP of MMA, polymerizations were performed with no vial headspace under air or under nitrogen for comparison and monitored over time (Figure 1). Given that 0.5 dram vials allowed for the reactions to be performed on a reasonable scale (8.60 mmol) with no vial headspace, a modified photoreactor was employed, which allowed for efficient stirring of these vials while employing the same light source used to investigate the effect of vial headspace on the reaction (see Supporting Information for more details). For the O-ATRP of MMA performed under air, pseudo first order kinetics were observed for monomer consumption over time (Figure 1A, left) and analysis of the of PMMA synthesized revealed linear growth of polymer molecular weight as a function of monomer conversion with measured M_n values in agreement with theoretical values (Figure 1A, right) and polymer ~ 1.2–1.3.

Conducting the O-ATRP of MMA under nitrogen using PC 1 and reagents which were purified rigorously to exclude air yielded similar results to the O-ATRP performed under air (Figure 1B). In particular, the polymerization performed under nitrogen proceeded with a similar rate (O-ATRP under air reached 77% conversion in 8 h while the reaction under nitrogen reached 74% conversion) and synthesized PMMA exhibiting similar (~ 1.2). However, performing the reaction under nitrogen led to better control over polymer M_n, as evidenced by a higher I^* of 94% (compared to the reaction performed under air which exhibited $I^* = 88\%$). Proton NMR analysis of precipitated PMMA synthesized under air or under nitrogen revealed no significant differences in polymer structure (Figures S7 and S8).

Temporal control was investigated for the O-ATRP of MMA performed under air using a pulsed irradiation experiment over the course of several days (Figure 2). Monomer

conversion was only observed during irradiation periods (Figure 2A) accompanied by a linear increase in polymer M_n as a function of conversion with polymer   remaining ~1.2 (Figures 2B, C). Removal of the light source halted the polymerization (for up to 22 h) with no further monomer conversion (Figure 2A), growth of polymer M_n (Figure 2B), or shift in the retention times of polymer GPC traces (Figure 2C). Comparison of polymer M_n,   , and GPC traces before and after dark periods revealed marginal differences in these data, indicating that air had no deleterious effects on the ability of PC **1** to (re)activate polymer chains in the presence of light (Figures 2A,B). Moreover, PC 1 was able to resume the polymerization after removing the light source for an extended period of time (16 h), suggesting that the PC exhibits some stability in the presence of air, albeit in the absence of light.

The reversible deactivation equilibrium established in O-ATRP enables the synthesis of polymers with high chain end group fidelity which can initiate subsequent polymerizations allowing for the synthesis of polymers with complex composition and architecture. To explore this feature in O-ATRP systems performed under air, matrix-assisted laser desorption/ ionization time-of-flight (MALDI–TOF) analysis (Figure S22) was performed on a PMMA macroinitiator synthesized under air (Table S3). Peaks in the MALDI–TOF spectrum were assigned to polymer with a DBMM-derived α-end group and either a bromide or hydrogen ω-end group. Presence of the bromide end group supports the reversible-deactivation mechanism, while presence of the polymers with hydrogen terminal groups indicates the occurrence of termination events involving hydrogen abstraction. To gain insight into the proportion of polymer chains bearing alkyl bromide chain end groups, the PMMA macroinitiator was introduced to either additional MMA or benzyl methacrylate (BnMA) using O-ATRP conditions (Figure 3A). Shorter retention times were observed for the GPC trace of the chain-extended PMMA compared to the PMMA macroinitiator (Figure 3B) accompanied by a higher measured M_n value (M_n = 8.2 kDa for the macroinitiator and M_n = 20.6 kDa after chain extension with MMA) and high I^* (I^* = 89%), indicating good bromide chain end group fidelity of the macroinitiator. Addition of BnMA to the PMMA macroinitiator using O-ATRP conditions under air allowed for the synthesis of a poly(MMA-*b*-BnMA) copolymer with high I^* (I^* = 89%), and   = 1.50, demonstrating control over the polymerization even at high conversion (94% conversion).

To gain further insight into the catalytic performance of core modified *N*-aryl phenoxazines in O-ATRP performed under air, five additional PCs (Table 2, PCs **2**–**6**) exhibiting a range of photophysical and redox properties (Tables S1 and S2) were investigated. In accordance with our previous results,[13] performing the O-ATRP of MMA under nitrogen using the modified photoreactor revealed that the PCs that exhibit stronger visible light absorption and more strongly reducing excited states (PCs **1**–**4**) synthesized PMMA with lower   and higher I^* than the other PCs explored (Table 2, runs 9–16, odd numbered runs). The evaluation of success for this trend is based on the linearity of growth of polymer M_n as a function of conversion and the ability of each PC to synthesize polymer with low   and high I^* throughout the polymerization. PCs **1**–**6** were able to mediate the O-ATRP of MMA under air in a controlled fashion as demonstrated by the linear growth of polymer M_n as a function of monomer conversion (Figures S12, S14, S16, S18, and S20) and the synthesis of

PMMA with high $I^* = 84–88\%$ and   ~ 1.2–1.3 (runs 9–20, even numbered runs). However, I^* was lower for the polymerizations performed under air compared to those performed under nitrogen for all PCs except **5** (on average I^* was ~5% lower for the O-ATRP performed under air and catalyzed by **1**–**4** and **6**), suggesting the presence of side reactions during the polymerizations performed under air.

In conclusion, O-ATRP performed under air and catalyzed by core modified *N*-aryl phenoxazines was found to proceed in a controlled fashion despite the potential deleterious effects of oxygen. Control over the polymerization using PC 1 was demonstrated by a linear growth of polymer M_n as a function of monomer conversion, the synthesis of PMMA with high I^* ($I^* = 88\%$ after 8 h) and   ~ 1.2, and the synthesis of block copolymers. Temporal control over O-ATRP performed under air was demonstrated using a pulsed-irradiation experiment carried out over the course of multiple days. In accordance with reports on the effects of air on Cu catalyzed ATRP systems, reduction of the volume of air in the reaction vial headspace was critical to the success of this procedure such that elimination of vial headspace led to the synthesis of polymeric material with the highest I^*. Investigation of five other PCs (**2**–**6**) in O-ATRP performed under air revealed that control over the polymerization under these conditions is not exclusive to PC **1**. In particular, all PCs explored were able to synthesize PMMA with   ~ 1.2–1.3 and $I^* = 84–99\%$. Trends in PC performance for O-ATRP performed under air followed those for the polymerizations performed under nitrogen with PC 1 exhibiting the best overall performance. In the O-ATRP reactions performed under air, I^* was consistently lower than the reactions performed under nitrogen for most of the PCs (**1**–**4** and **6**), suggesting the presence of additional side reactions in the presence of air. Future work is aimed at understanding the mechanisms enabling these O-ATRP reactions to proceed in a controlled fashion under air without the addition of exogenous reagents.

Supplementary Material

Refer to Web version on PubMed Central for supplementary material.

ACKNOWLEDGMENTS

REFERENCES

(1). Chen M; Zhong M; Johnson JA Light-Controlled Radical Polymerization: Mechanisms, Methods, and Applications. Chem. Rev 2016, 116, 10167–10211. [PubMed: 26978484]

(2). Corrigan N; Shanmugam S; Xu J; Boyer C Photocatalysis in organic and polymer synthesis. Chem. Soc. Rev 2016, 45, 6165–6212. [PubMed: 27819094]

(3). Discekici EH; Pester CW; Treat NJ; Lawrence J; Mattson KM; Narupai B; Toumayan EP; Luo Y; McGrath AJ; Clark PG; Read de Alaniz J.; Hawker CJ Simple Benchtop Approach to Polymer Brush Nanostructures Using Visible-Light-Mediated Metal-Free Atom Transfer Radical Polymerization. ACS Macro Lett 2016, 5, 258–262.

(4). Ligon SC; Hu ar B; Wutzel H; Holman R; Liska R Strategies to Reduce Oxygen Inhibition in Photoinduced Polymerization. Chem. Rev 2014, 114, 557–589. [PubMed: 24083614]

(5). Flory PJ In Principles of Polymer Chemistry; Cornell University Press: New York, 1995; p 168.

(6). Turro NJ; Ramamurthy V; Scaiano JC In Modern Molecular Photochemistry of Organic Molecules; University Science Books: Mill Valley, CA, 2010; p 1001.

(7). Yeow J; Chapman R; Gormley AJ; Boyer C Up in the air: oxygen tolerance in controlled/living radical polymerization. Chem. Soc. Rev 2018, 47, 4357–4387. [PubMed: 29718038]

(8). Miyake GM; Theriot JC Perylene as an Organic Photocatalyst for the Radical Polymerization of Functionalized Vinyl Monomers through Oxidative Quenching with Alkyl Bromides and Visible Light. Macromolecules 2014, 47, 8255–8261.

(9). Theriot JC; Lim C-H; Yang H; Ryan MD; Musgrave CB; Miyake GM Organocatalyzed atom transfer radical polymerization driven by visible light. Science 2016, 352, 1082–1086. [PubMed: 27033549]

(10). Ryan MD; Theriot JC; Lim C-H; Yang H; Lockwood AG; Garrison NG; Lincoln SR; Musgrave CB; Miyake GM Solvent Effects on the intramolecular charge transfer character of N,N-diaryl dihydrophenazine catalysts for organocatalyzed atom transfer radical polymerization. J. Polym. Sci., Part A: Polym. Chem 2017, 55, 3017–3027.

(11). Lim C-H; Ryan MD; McCarthy BG; Theriot JC; Sartor SM; Damrauer NH; Musgrave CB; Miyake GM Intramolecular Charge Transfer and Ion Pairing in N,N-Diaryl Dihydrophenazine Photoredox Catalysts for Efficient Organocatalyzed Atom Transfer Radical Polymerization. J. Am. Chem. Soc 2017, 139, 348–355. [PubMed: 27973788]

(12). Theriot JC; Miyake GM; Boyer CA N,N-Diaryl Dihydrophenazines as Photoredox Catalysts for PET-RAFT and Sequential PET-RAFT/O-ATRP. ACS Macro Lett 2018, 7, 662–666. [PubMed: 30705782]

(13). Pearson RM; Lim C-H; McCarthy BG; Musgrave CB; Miyake GM Organocatalyzed Atom Transfer Radical Polymerization using N-Aryl Phenoxazines as Photoredox Catalysts. J. Am. Chem. Soc 2016, 138, 11399–11407. [PubMed: 27554292]

(14). McCarthy BG; Pearson RM; Lim C-H; Sartor SM; Damrauer NH; Miyake GM Structure-Property Relationships for Tailoring Phenoxazines as Reducing Photoredox Catalysts. J. Am. Chem. Soc 2018, 140, 5088–5101. [PubMed: 29513533]

(15). Sartor SM; McCarthy BG; Pearson RM; Miyake GM; Damrauer NH Exploiting Charge-Tranfer States for Maximizing Intersystem Crossing Yields in Organic Photoredox Catalysts. J. Am. Chem. Soc 2018, 140, 4778–4781. [PubMed: 29595966]

(16). Treat NJ; Sprafke H; Kramer JW; Clark PG; Barton BE; Read de Alaniz J.; Fors BP; Hawker CJ Metal-Free Atom Transfer Radical Polymerization. J. Am. Chem. Soc 2014, 136, 16096–16101. [PubMed: 25360628]

(17). Pan X; Lamson M; Yan J; Matyjaszewski K Photoinduced Metal-Free Atom Transfer Radical Polymerization of Acrylonitrile. ACS Macro Lett 2015, 4, 192–196.

(18). Pan X; Fang C; Fantin M; Malhotra N; So WY; Peteanu LA; Isse AA; Gennaro A; Liu P; Matyjaszewski K Mechanism of Photoinduced Metal-Free Atom Transfer Radical Polymerization: Experimental and Computational Studies. J. Am. Chem. Soc 2016, 138, 2411–2425. [PubMed: 26820243]

(19). Liu X; Zhang L; Cheng Z; Zhu X Metal-free photoinduced electron transfer–atom transfer radical polymerization (PET–ATRP) via a visible light organic photocatalyst. Polym. Chem 2016, 7, 689–700.

(20). Kutahya C; Aykac FS; Yilmaz G; Yagci Y LED and visible light-induced metal free ATRP using reducible dyes in the presence of amines. Polym. Chem 2016, 7, 6094–6098.

(21). Allushi A; Jockusch S; Yilmaz G; Yagci Y Photoinitiated Metal-Free Controlled/Living Radical Polymerization Using Polynuclear Aromatic Hydrocarbons. Macromolecules 2016, 49, 7785–7792.

(22). Allushi A; Kutahya C; Aydogan C; Kreutzer J; Yilmaz G; Yagci Y Conventional Type II photoinitiators as activators for photoinduced metal-free atom transfer radical polymerization. Polym. Chem 2017, 8, 1972–1977.

(23). Kutahya C; Allushi A; Isci R; Kreutzer J; Ozturk T; Yilmaz G; Yagci Y Photoinduced Metal-Free Atom Transfer Radical Polymerization Using Highly Conjugated Thienothiophene Derivatives. Macromolecules 2017, 50, 6903–6910.

(24). Huang Z; Gu Y; Liu X; Zhang L; Cheng Z; Zhu X Metal-Free Atom Transfer Radical Polymerization of Methyl Methacrylate with ppm Level of Organic Photocatalyst. Macromol. Rapid Commun 2017, 38, 1600461.

(25). Theriot JC; McCarthy BG; Lim C-H; Miyake GM Organocatalyzed Atom Transfer Radical Polymerization: Perspectives on Catalyst Design and Performance. Macromol. Rapid Commun 2017, 38, 1700040.

(26). Pan X; Fantin M; Yuan F; Matyjaszewski K Externally controlled atom transfer radical polymerization. Chem. Soc. Rev 2018, 47, 5457. [PubMed: 29868657]

(27). Liarou E; Whitfield R; Anastasaki A; Engelis NG; Jones GR; Velonia K; Haddleton DM Copper-Mediated Polymerization without External Deoxygenation or Oxygen Scavengers. Angew. Chem., Int. Ed 2018, 57, 8998–9002.

(28). Matyjaszewski K; Coca S; Gaynor SG; Wei M; Woodworth BE Controlled Radical Polymerization in the Presence of Oxygen. Macromolecules 1998, 31, 5967–5969.

(29). Ryan MD; Pearson RM; French TA; Miyake GM Impact of Light Intensity on Control in Photoinduced Organocatalyzed Atom Transfer Radical Polymerization. Macromolecules 2017, 50, 4616–4622. [PubMed: 29551839]

(30). Ramsey BL; Pearson RM; Beck LR; Miyake GM Photoinduced Organocatalyzed Atom Transfer Radical Polymerization Using Continuous Flow. Macromolecules 2017, 50, 2668–2674. [PubMed: 29051672]

(31). Discekici EH; Amant AH St.; Nguyen SN; Lee I-H; Hawker CJ; Read de Alaniz J. Endo and Exo Diels-Alder Adducts: Temperature-Tunable Building Blocks for Selective Chemical Functionalization. J. Am. Chem. Soc 2018, 140, 5009–5013. [PubMed: 29613783]

(32). Buss BL; Beck LR; Miyake GM Synthesis of star polymers using organocatalyzed atom transfer radical polymerization through a core-first approach. Polym. Chem 2018, 9, 1658–1665. [PubMed: 29628993]
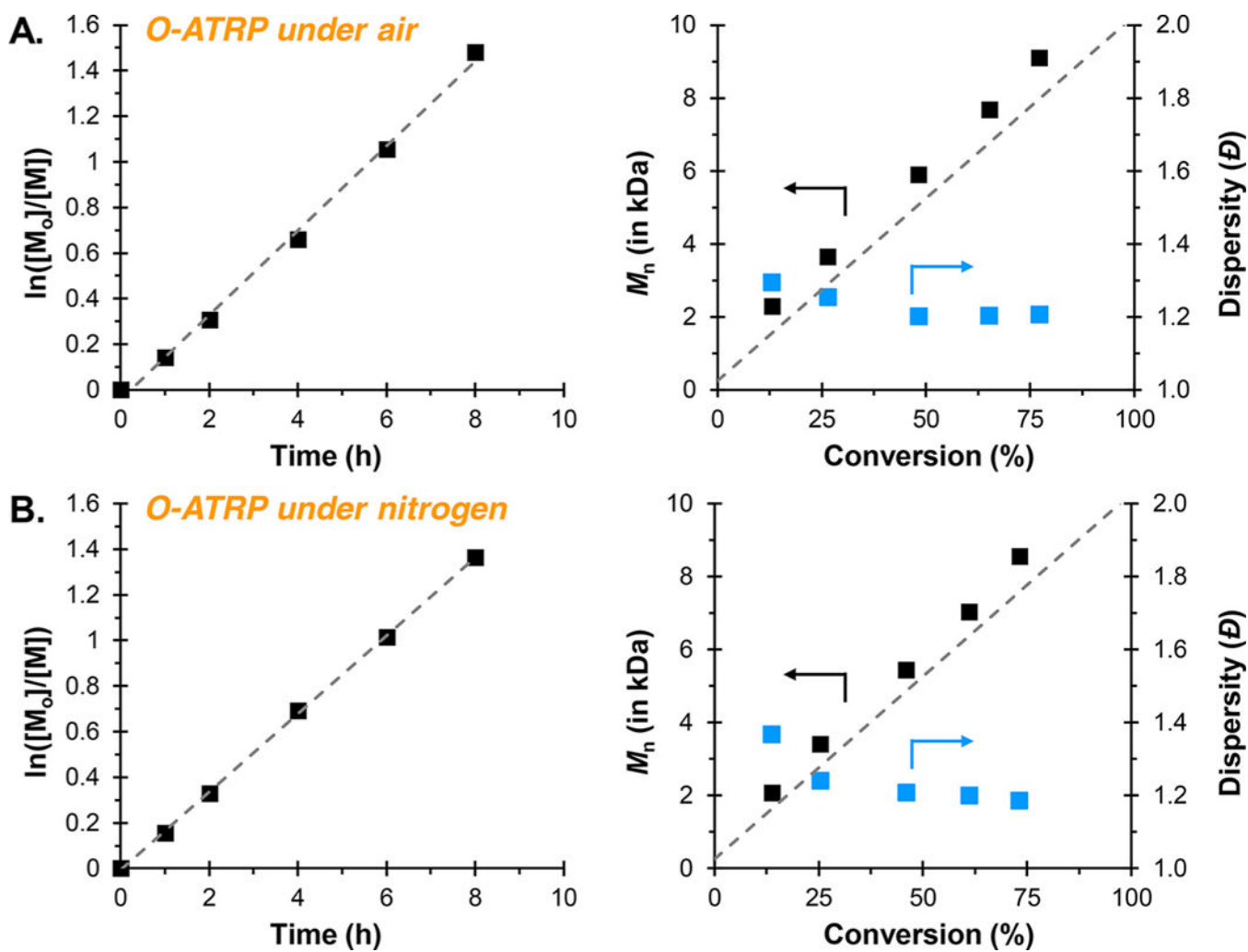
Author Manuscript

Author Manuscript

Author Manuscript

Author Manuscript

Figure 1.

Plots of the natural log of monomer consumption as a function of time (left) for the O-ATRP of MMA mediated by 1 under air (A) or under nitrogen (B) with a [1000]:[10]:[1] ratio of MMA:DBMM:PC 1. Plots of growth of the experimentally measured M_n as a function of monomer conversion (right, black squares) with theoretical values (gray, dashed line). Dispersity of the PMMA at each M_n is shown (blue squares).
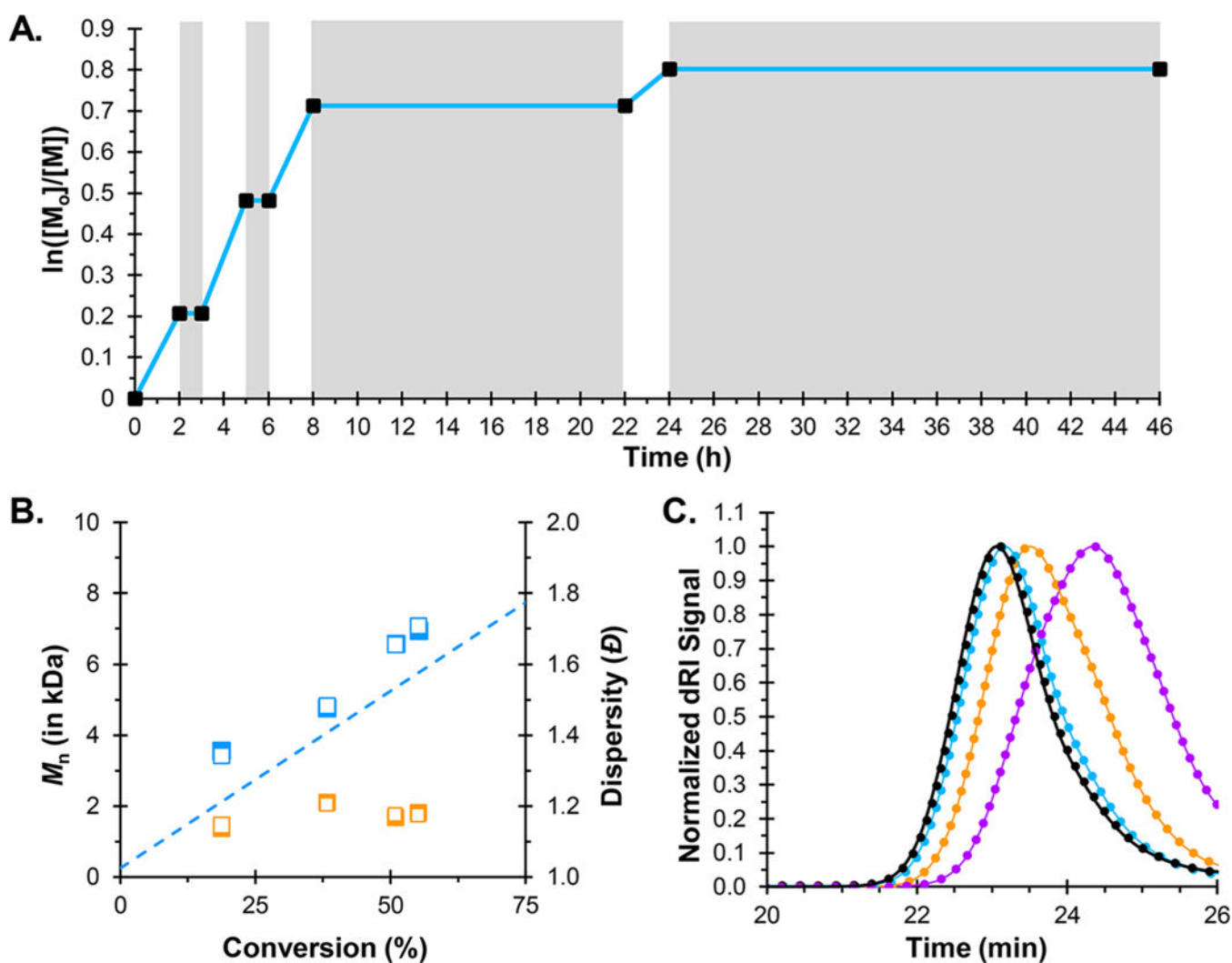
Figure 2.

Plot of growth of the natural log of monomer consumption as a function of time for a pulsed irradiation experiment conducted under air (A). Plot of growth of the experimentally measured M_n as a function of monomer conversion with theoretical M_n values (B, filled, blue squares are M_n values directly after irradiation while open markers are data directly after dark periods; blue dashed line shows theoretical M_n values). Dispersity of the PMMA at each M_n are shown (filled, orange squares are data directly after irradiation while open markers are data directly after dark periods). Gel permeation chromatography traces of PMMA synthesized during the pulsed irradiation experiment (C, traces with dotted lines are after each irradiation period and traces with bold lines are after dark periods).
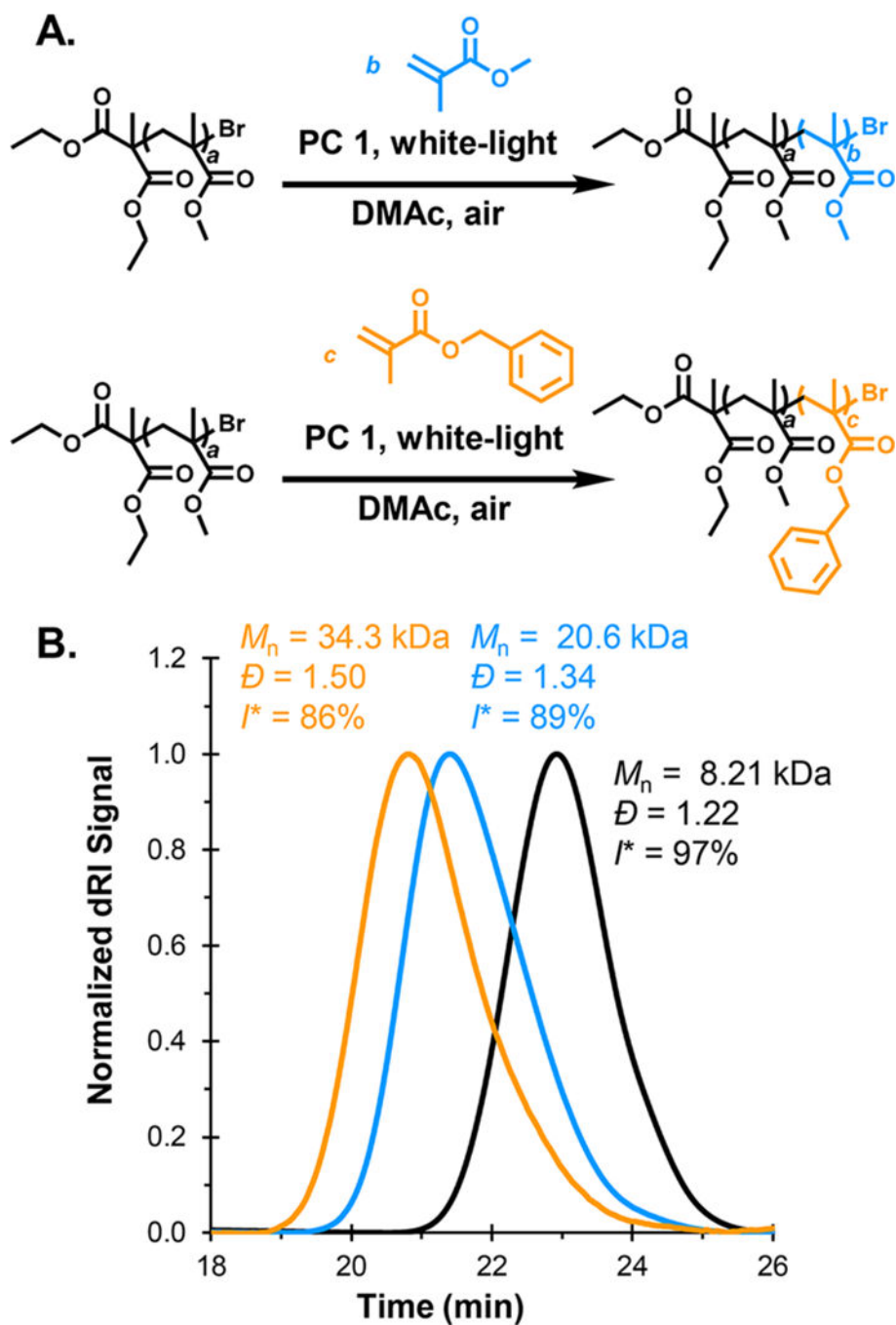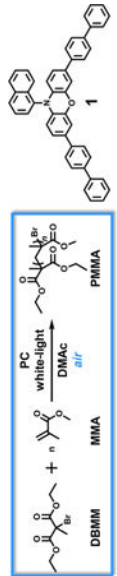
Figure 3.
Chain extension polymerizations with MMA (A, top) or BnMA (A, bottom) performed under air from a PMMA macroinitiator synthesized via O-ATRP under air. GPC traces of the PMMA macroinitiator synthesized under air before (B, black trace) and after addition of MMA (B, blue trace) or BnMA (B, orange trace).

Table 1.

Results of the O-ATRP of MMA with Varied Reaction Vial Headspace[a]

run no.	vial headspace of air (mL)	time (h)	convn (%)	$M_{n,th}$ (kDa)	M_n (kDa)	M_w (kDa)	(M_w/M_n)	I^* $(M_{n,th}/M_n \times 100)$
1	18.2	24	36	3.9	7.6	14.5	1.90	50
2	5.55	24	69	7.1	9.4	11.8	1.25	75
3	3.71	24	77	8.0	10.5	12.8	1.22	76
4	1.86	8	53	5.5	7.3	8.8	1.21	76
5	0	8	68	7.0	8.1	9.8	1.22	87
6	0	26	95	9.8	11.3	13.2	1.18	87
7[b]	0	24	7	0.9	–	–	–	–
8[c]	0	24	0	0	–	–	–	–
9[d]	0	8	36	3.9	49.5	84.8	1.71	8

[a]Reaction scheme for the O-ATRP of MMA performed under air (blue box) and structure of PC 1 (top right). The O-ATRP was performed with a [1000]:[10]:[1] ratio of MMA: diethyl 2-bromo-2-methylmalonate (DBMM): PC 1 (see Supporting Information for more details).
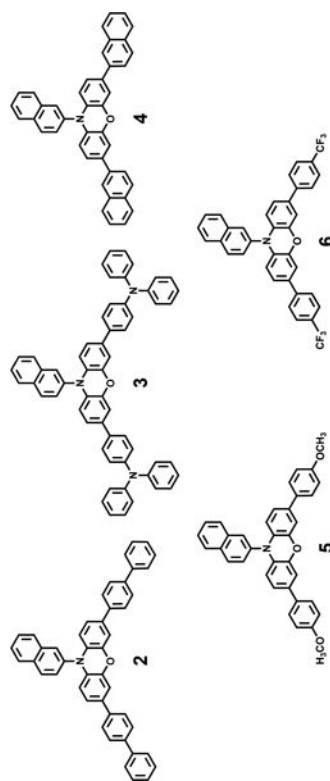
[b]Reaction performed without PC.

[c]Reaction performed without light.

[d]Reaction performed without initiator.

Table 2.

Results of the O-ATRP of MMA under Air or Nitrogen Mediated by PCs 1–6[a]

run no.	PC	atmosphere	time (h)	convn (%)	$M_{n,th}$ (kD$_a$)	M_n (kD$_a$)	M_w (kD$_a$)	(M_w/M_n)	I* ($M_{n,th}/M_n \times 100$)
9	1	N$_2$	8	74	7.7	8.2	9.8	1.19	94
10	1	air	8	77	8.0	9.1	11.0	1.21	88
11	2	N$_2$	8	63	6.6	6.8	8.7	1.29	97
12	2	air	8	73	7.6	8.6	10.2	1.19	88
13	3	N$_2$	8	64	6.7	7.6	9.2	1.20	87
14	3	air	8	52	5.5	6.5	7.6	1.16	84
15	4	N$_2$	8	60	6.2	6.7	8.3	1.24	93
16	4	air	8	63	6.6	7.9	9.5	1.21	84
17	5	N$_2$	8	60	6.3	7.3	9.4	1.28	86
18	5	air	8	69	7.2	7.7	10.3	1.33	93
19	6	N$_2$	8	67	6.9	7.0	8.6	1.22	99
20	6	air	8	71	7.4	8.2	10.1	1.23	89

[a]The O-ATRP of MMA was performed with a [1000]:[10]:[1] ratio of MMA:DBMM:PC in 1:1 of MMA:DMAc v/v with 0.92 mL (8.60 mmol) of MMA in a vial with no headspace. See Supporting Information for more details.